Frontiers in Bioscience Landmark

Front. Biosci. (Landmark Ed) **2025**; 30(10): 45355
https://doi.org/10.31083/FBL45355

Original Research

Cathepsin S Contributes to Bladder Fibrosis Following Bladder Outlet Obstruction via IL-6 Trans-signaling

Mengchen Yang[1,†], Xilei Liu[1,†], Hong Wang[1], Tianyu Shen[2,*], Liang Wang[1,*]

[1]Department of Urology, Tianjin Medical University General Hospital, 300052 Tianjin, China
[2]School of Medicine, Nankai University, 300071 Tianjin, China
*Correspondence: shentianyu@nankai.edu.cn (Tianyu Shen); tjzyymnwk@163.com (Liang Wang)
[†]These authors contributed equally.

Academic Editor: Esteban C. Gabazza
Submitted: 28 July 2025 Revised: 18 September 2025 Accepted: 10 October 2025 Published: 31 October 2025

Abstract

Background: Bladder outlet obstruction (BOO) frequently accompanies benign prostate hyperplasia (BPH) in aging males and often leads to bladder fibrosis, a secondary pathological change that contributes to bladder dysfunction. The role of Cathepsin S (CTSS), a cysteine protease associated with immune responses, in this process remains to be fully elucidated. **Methods**: Bladder tissues from BOO model mice were analyzed using microarray profiling, followed by Gene Ontology (GO) and pathway enrichment analyses. Candidate genes, including *CTSS*, C-X-C Motif Chemokine Ligand 17 (CXCL17), and Angiopoietin Like 7 (ANGPTL7), were identified. CTSS was selected for further investigation based on its association with fibrotic processes. The functional role of CTSS in smooth muscle cell hypertrophy and fibrosis was verified both *in vivo* and *in vitro*. A co-culture system of smooth muscle cells and monocyte–macrophages was used to explore the underlying mechanism. **Results**: Microarray and bioinformatic analysis identified CTSS as a key candidate gene associated with immune response in BOO-induced bladder fibrosis. CTSS expression was upregulated in BOO bladders and was demonstrated to promote smooth muscle cell hypertrophy and fibrotic changes. Mechanistically, CTSS mediated proteolytic cleavage of the interleukin-6 receptor (IL-6R) on immune cells, generating soluble IL-6R (sIL-6R). This process facilitated IL-6 trans-signaling, which in turn promoted smooth muscle cell hypertrophy and exacerbated bladder fibrosis. **Conclusions**: These findings indicate that CTSS contributes to BOO-induced bladder dysfunction and fibrosis by activating IL-6 trans-signaling through cleavage of IL-6R. CTSS may represent a potential therapeutic target for mitigating bladder fibrosis in BPH.

Keywords: bladder outlet obstruction; benign prostate hyperplasia; cathepsin S; interleukin-6; fibrosis

1. Introduction

Bladder outlet obstruction (BOO) is a clinically urological problem that is secondary to benign prostate hyperplasia (BPH) in aging males. Persistent BOO may cause the progression of lower urinary tract symptoms (LUTS), which can severely interfere with the quality of life [1,2]. During the development of BOO, bladder smooth muscle undergoes hypertrophy in response to increased urethral resistance, which ultimately progresses to bladder remodeling and fibrosis at the decompensation stage [3]. Decompensated bladder tissue fibrosis represents a critical pathological process and occurs in the majority of BOO patients.

The progression of fibrosis is characterized by excessive deposition of extracellular matrix (ECM) and bladder smooth muscle cell (BSMC) hyperplasia, leading to BSMC dysfunction and decreased bladder compliance [4]. As demonstrated in a previous study, inflammation and transforming growth factor-beta (TGFβ) signaling play central roles in bladder tissue fibrosis. Moreover, the growth factor signaling pathway has been found to be activated in all BOO patients [5]. Tetrahedral framework nucleic acids have been shown to inhibit bladder remodeling by deactivating STAT and TGFβ/Smad pathway [6].

Cathepsin S (CTSS), a lysosomal protease and a member of the cysteine proteases, is present in the cytoplasm of antigen-presenting cells, B cells, and monocyte–macrophages. It participates in a variety of pathological processes such as cancers, arthritis, osteoporosis, cardiovascular disease, and chronic obstructive pulmonary disease [7]. A recent study has shown that CTSS overexpression accelerated extracellular matrix remodeling and pulmonary fibrosis [8]. In addition, CTSS increased the deposition of ECM and activated the TGFβ/Smad signaling pathway, which promotes the development of renal fibrosis [9]. However, few studies have shown the relationship between CTSS and bladder remodeling and fibrosis.

In this study, we investigated the pathological changes associated with bladder remodeling following BOO and analyzed differential gene expression throughout this process. CTSS exhibited the most significant change in all models and was therefore selected for further investigation. Inhibition of CTSS ameliorated BOO-induced bladder dysfunction and fibrosis. Furthermore, the mechanism of the selected gene, CTSS, in bladder fibrosis was also studied.

2. Methods and Materials

2.1 Animals

All procedures involving animals in this study complied with the NIH Guide for the Care and Use of Laboratory Animals and were approved by the Animal Care and Use Committee of Tianjin Medical University (approval No. IRB2024-DWFL-173). Male C57BL/6J mice, weighing between 22 and 24 g, were obtained from Vital River Laboratory Animal Technology Co., Ltd (Beijing, China). and maintained in the animal facility of Tianjin Medical University General Hospital at 22–25 ℃ temperature and 50% relative humidity under a 12 h light/dark cycle. All animals had access to food and water.

The mice were subjected to microsurgical creation of BOO under anesthesia using isoflurane essentially as described [10]. Briefly, mice were anesthetized with 1.5% isoflurane and placed in a supine position with a 1–2 cm incision to expose the urethrovesical junction. A 0.5-mm inner diameter polyethylene tube was placed around the bladder neck, and a 3-0 polypropylene suture was used to tie gently around the bladder neck and then draw out the catheter. Then the incision was closed and disinfected. Mice were anesthetized with 1.5% isoflurane and euthanized via cervical dislocation at day 21 post-operation. Some parts of the bladder tissues were collected immediately for histology or immunochemistry, and the remaining tissues were snap-frozen in liquid nitrogen for performing microarray, qPCR, or western blotting.

In vivo siRNA transfection was performed using Lipofectamine-3000 (Thermo Fisher Scientific, Waltham, MA, USA). Both siRNA-CTSS (0.5 nmol, RiboBio, Guangzhou, China) and siRNA-control (0.5 nmol, RiboBio) were complexed with an equal volume of Lipofectamine-3000 prior to delivery. The mixed solutions were injected through the tail vein daily. The BOO model was administered immediately post-transfection.

2.2 Cell Culture

Mice smooth muscle cell line (mBSMC) and macrophage cell line (RAW264.7) were purchased from Yipu Biotechnology (Wuhan, China) and cultured in DMEM-basic medium (Gibco, Waltham, MA, USA) with 10% FBS and 1% penicillin/streptomycin (Thermo Fisher Scientific). The interaction between mBSMC and RAW264.7 was detected by a Transwell system (Corning Corporation, Corning, NY, USA). mBSMC were inoculated into the lower chamber, while RAW264.7 cell was cultivated in the upper chamber of the Transwell system. The cells were maintained in a culture chamber (Thermo Fisher Scientific) at 37 ℃ with 5% CO_2. We incubated the cells with 10 ng/mL TGFβ (HY-P78360, MedChem Express LLC, Monmouth Junction, NJ, USA) for 15 minutes to induce cell hypertrophy. *In vivo* siRNA transfection was performed using Lipofectamine-3000 (L3000075, Thermo Fisher Scientific). Both siRNA-CTSS (0.5 nmol, RiboBio) and siRNA-control (0.5 nmol, RiboBio) were complexed with an equal volume of Lipofectamine-3000 prior to delivery and added to the culture medium for 5 h. All cell lines were validated by short tandem repeat (STR) profiling and tested negative for mycoplasma.

2.3 Void Stain on Paper (VSOP)

The mice were placed in individual metabolic cages for 1 h with an underlying Whatman filter paper, and food and water were obtained ad libitum. The filter paper sheets were then imaged using UV light. The number and pattern of voids were noted, and the area of each voiding stain was measured using Image J (v1.8.0, NIH, Bethesda, MD, USA). The volume of urine was onverted from the stain area by using a standard curve. Sporadic noncircular small-diameter urine spots were excluded.

2.4 Gene Microarray Testing

Total RNA was extracted from the samples using standard extraction methods. Total RNA (with the addition of PolyA control), cDNA first-strand and second-strand were synthesized, and cRNA was synthesized by *in vitro* transcription. After purification and quantification of cRNA, cRNA was diluted to 625 ng/µL for subsequent experiments. After purification of the synthesized 2nd-cycle single-stranded cDNA, 5.5 µg of sscDNA was diluted to 31.2 µL with enzyme-free water for subsequent fragmentation and labeling. The fragmented and labeled samples are added to the corresponding microarrays and placed into the GeneChip Hybridization Oven 645 (Affymetrix, Santa Clara, CA, USA) for hybridization at a specific temperature and speed; after reaching the specified time, the microarrays were eluted using the GeneChip Fluidics Station 450 (Affymetrix, Santa Clara, CA, USA) according to the corresponding protocol. After completion, the GeneChip 3000 7G scanner (Affymetrix, Santa Clara, CA, USA) was used for scanning. The scanner captures the fluorescence signal and converts the signal by GCOS software to obtain the signal value of each probe and generate a CEL file. False Discovery Rate (FDR) correction for high-throughput gene data.

2.5 Histological Analysis and Immunohistochemical Staining

The bladder tissues were submerged overnight in 4% paraformaldehyde and then embedded in paraffin, and 5 µm sections were sliced. Masson's trichrome staining method was used to evaluate the extent of bladder tissue fibrosis. For immunohistochemical (IHC) staining, bladder sections were blocked with 0.3% Triton X-100 (Solarbio, Beijing, China) and 3% albumin bovine V (biotopped, Beijing, China) and incubated overnight with antibodies as follows: Anti-alpha smooth muscle Actin 2 (ACTA2) (ab5694, Abcam, Cambridge, UK), Collegen-I (Col-I) (ab270993, Abcam), Col-III (22734-1-AP, Protein-

tech, Chicago, IL, USA). Following incubation with a secondary antibody, 3,3-diaminobenzidine (Gene Tech) was used as a substrate, and re-staining was performed with hematoxylin (Solarbio). These slices were observed and imaged using a DM500 light microscope (Leica, Wetzlar, Germany). The results of immunochemistry were measured by using the Image J software (v1.8.0, NIH). A total of 5 randomly selected fields were captured and analyzed. For immunofluorescence (IF) staining, the cell creep was placed in a cell culture dish and cleaned 3 times using PBS. After cleaning, the cells were fixed at room temperature with 4% paraformaldehyde for 20 minutes and then rinsed with PBS 3 times. Subsequently, slides were treated with 5% BSA for 30 minutes at room temperature to block nonspecific staining. Slides were incubated with different primary antibodies (Abcam) overnight at 4 °C. On the second day, slides were cleaned with PBS 3 times and incubated with the corresponding secondary antibody (Abcam) for 1 hour at room temperature. Finally, the slides were washed with PBS 3 times, and the slides were sealed. The nuclei were counterstained with DAPI. The slides were used to observe and quantify with a DMILLED immunofluorescence microscope (Leica). The fluorescent intensity was determined using Image J (v1.8.0, NIH). A total of 5 randomly selected fields were captured and analyzed.

2.6 Western Blotting

The bladder tissues were placed in Radio Immunoprecipitation Assay (RIPA) Lysis buffer, which was sonicated for 10 minutes and then centrifuged at 13,000 rpm for 15 minutes at 4 °C. Protein concentration was determined by the kit (Solarbio). Equal amounts of proteins were separated on the gel by sodium dodecyl sulfate - polyacrylamide gel electrophoresis and then transferred to Polyvinylidene Fluoride membranes. The membranes were then blocked in 5% skim milk and reacted overnight at 4 °C with different primary antibodies: IL-6 (AMC0864, Invitrogen, Carlsbad, CA, USA), interleukin-6 receptor (IL-6R) (ab83053, Abcam), CTSS (ab232740, Abcam), ACTA2 (ab5694, Abcam), Actin (ab8226, Abcam), Col-I (ab270993, Abcam), Col-III (22734-1-AP, Proteintech), CXCL17 (MA5-24157, Invitrogen), Tubulin (11224-1-ap, Proteintech), Angptl7 (PA5-36575, Invitrogen). After incubation with secondary antibodies coupled to horseradish peroxidase membranes, they were observed using an enhanced chemiluminescence detection kit (Millipore Sigma, Burlington, MA, USA), and the mean pixel density of protein bands was quantified by ImageJ software (v1.8.0, NIH) and was standardized to GAPDH or tubulin.

2.7 RNA Extraction and Quantitative Real-time PCR

RT-qPCR was performed to detect cytokine RNA levels in bladder tissues. Total RNA was extracted using the kit (Accurate Biology, Changsha, China). The obtained RNA samples were then reverse-transcribed into cDNA using the PrimeScript RT reagent Kit (Takara, Kusatsu, Japan). Finally, quantitative PCR was performed on an Applied Biosystems 7300 Plus using a Direct TB Green qPCR kit (Takara). Results were normalized using GAPDH gene expression and expressed as relative expression values. The primer sequences were as follows:

① CTSS:

Primer-F: 5′ TGACGAGGATGCCCTGAAAGA 3′

Primer-R: 5′ GTCCCATAGCCAACCACAAGA 3′

② CXCL17:

Primer-F: 5′ AAAAGCACCACAGGAAGTCGC 3′

Primer-R: 5′ TCTTGTAGGGTAAACAGAAGGCATAA 3′

③ Angptl7:

Primer-F: 5′ TCTACCATAACAACACCGTCTTCAGC 3′

Primer-R: 5′ GATGCCATCCATGTGCTTTCG 3′

2.8 Enzyme-Linked Immunosorbent Assay (ELISA)

The bladder samples were homogenized according to the manufacturer's protocol. Inflammatory factors were detected in the bladder samples using ELISA kits for CTSS, IL-6, and soluble IL-6R (sIL-6R) (KND, Wenzhou, China). The measured OD values were converted into concentration values.

2.9 Statistical Analysis

All results were expressed as mean ± standard deviation (SD). Student's *t*-test or one-way analysis of variance (ANOVA) test followed by Tukey's post hoc test were used among the groups. The Statistical Package for the Social Sciences (SPSS) software version 26.0 (IBM Corporation, Armonk, NY, USA) was used to conduct the statistical analysis. A *p*-value less than 0.05 was considered significant.

3. Result

3.1 Bladder Dysfunction and Fibrosis Following Bladder Obstruction

To identify the pathological change of mice's bladder post-obstruction, we established an animal model using the Leadbetter operation and obtained the result of bladder function change in mice by observing urination behavior with VSOP. The results showed a dramatic decrease in urination volume after the obstruction occurred, which, in particular, started on day 7 post-obstruction (64.018 ± 94.431 µL vs control 345.2 ± 161.339 µL), and reached its lowest point by day 28 (6.878 ± 12.441 µL vs control 468.348 ± 109.671 µL) (Fig. 1A). Furthermore, ladder tissues were collected on the 28th day after obstruction. The Masson's staining and IHC results indicated the development of bladder fibrosis, along with elevated levels of fibrogenic or hypertrophy factor ACTA2, Col-I, and Col-III in the obstruction group (Fig. 1B–E). We carried out *in vitro* studies using

bladder smooth muscle cells, and the IF results showed that after TGFβ stimulation, significant hypertrophy of bladder smooth muscle cells was observed (Fig. 1F,G).

3.2 Differential Protein Expression Changes Following Bladder Obstruction

The volcano plot displayed the distribution of differential genes, with a total of 541 genes up-regulated and 943 genes down-regulated in the Obs group compared to the SHAM group (Fig. 2A). The heatmap showed the differential gene clustering analysis (Fig. 2B). Subsequent Gene Ontology (GO) enrichment analysis revealed that the up-regulated genes were concentrated in the functions of the innate immune response, immune system process, and cellular response to interferon-beta (Fig. 2C). Among these differential genes, we focused on the top ten most significantly upregulated genes in this Obs group (Fig. 2D). Combining the results of GO analysis with literature reports, we identified CTSS, CXCL17, and ANGPTL7 as candidate genes because they are all associated with immune response. We checked the expression level of selected proteins with qPCR, and the results indicated that CTSS, CXCL17, and ANGPTL7 increased dramatically after obstruction (Fig. 3A). We again examined the expression of these three candidate proteins in bladder tissues of mice with bladder obstruction. Western blot results showed that CTSS was most significantly upregulated compared to the control group; the level increased approximately nine-fold (Fig. 3B,C). Consistent with these *in vivo* findings, *in vitro* experiments demonstrated that CTSS expression was markedly up-regulated along with ACTA2 in bladder smooth muscle cells following TGFβ stimulation (Fig. 3D,E).

3.3 CTSS Participated in Bladder Dysfunction and Fibrosis Following BOO

To study the effect of CTSS on the mice bladder, VSOP showed that, compared with the obstruction group treated with siCTSS, the urine volume of the obs/siCTSS group starting from the 7th day following BOO. Particularly, the improvements were most significant on day 28 (123.956 $\pm$ 36.233 µL vs obs 24.878 $\pm$ 25.899 µL) and day 56 (82.256 $\pm$ 61.788 µL vs obs 18.386 $\pm$ 16.509 µL) (Fig. 4A). Masson's staining showed that the fibrosis condition improved when CTSS was suppressed (Fig. 4B). Furthermore, we performed IHC and Western blot on proteins from bladder tissues of various groups of mice, and the results showed that the expression of ACTA2 and Col-I, Col-III decreased due to down-regulation of CTSS in IHC and western blotting (Fig. 4B–G). All of these results indicated that CTSS induced bladder dysfunction and fibrosis following BOO.

3.4 CTSS Contributed to Smooth Muscle Cells' Hypertrophy With Monocyte–Macrophages' Participation

Our results demonstrated that the expression levels of CTSS were elevated in both TGFβ-stimulated smooth muscle cells (SMCs) and TGFβ-stimulated SMCs/monocyte–macrophages. For ACTA2, expression increased under both conditions; a substantial elevation was observed only in the presence of monocyte–macrophages existed (Fig. 5A,B). The upregulation of CTSS was abolished by siCTSS treatment; however, the most pronounced reduction in ACTA2 expression occurred when SMCs were co-cultured with monocyte–macrophages (Fig. 5C,D). Additionally, we also observed a reversal of TGFβ-induced SMCs hypertrophy following co-culturing with monocyte–macrophages and treated with siCTSS (Fig. 5E,F).

3.5 CTSS Affected Bladder Function via CTSS/sIL-6R/IL-6 After Bladder Obstruction

The expression levels of both CTSS and IL-6 in the cell supernatant were increased in TGFβ-stimulated SMCs (CTSS: 955.437 $\pm$ 16.315 pg/mL vs control 377.7 $\pm$ 7.231 pg/mL; IL-6: 155.143 $\pm$ 3.272 pg/mL vs control 19.183 $\pm$ 2.225 pg/mL) and in TGFβ stimulated SMCs/monocyte–macrophages (CTSS: 983.767 $\pm$ 27.134 pg/mL vs control 402.943 $\pm$ 34.184 pg/mL; IL-6: 198.08 $\pm$ 7.931 pg/mL vs control 54.757 $\pm$ 1.114 pg/mL) (Fig. 6A,B). In contrast, elevated levels of sIL-6R in supernatant were observed only in TGFβ SMCs/monocyte–macrophages (148.653 $\pm$ 2.551 pg/mL vs control 52.217 $\pm$ 4.11 pg/mL) (Fig. 6C). Conversely, when we blocked ADAM17 (a canonical protein that promotes the generation of sIL-6R) in the co-culture system, no significant effect was observed. By comparison, CTSS was identified as the primary mediator in this process (**Supplementary Fig. 1**). When CTSS expression was reduced using siCTSS, IL-6 levels remained unchanged in both the stimulated SMCs alone and the stimulated co-cultured group (Fig. 6D,E). However, sIL-6R expression decreased significantly only in the stimulated co-cultured group (115.52 $\pm$ 5.133 pg/mL vs control 181.11 $\pm$ 6.154 pg/mL) (Fig. 6F). Results from *in vivo* experiments in mice further confirmed this signaling pathway (Fig. 6G–I). These findings indicate that sIL-6R/IL-6 signaling is up-regulated after bladder obstruction and that CTSS knockdown inhibits this signaling axis. To block sIL-6R/IL-6 trans-signaling, we treated BOO mice daily with sgp130FC (0.5 mg/kg). The VSOP results showed improved bladder function on Day 21 (132.714 $\pm$ 32.118 µL vs obs 27.248 $\pm$ 21.324 µL) and Day 28 (92.713 $\pm$ 52.641 µL vs obs 16.267 $\pm$ 13.352 µL) (Fig. 7A). Bladder sensitivity was also improved (Fig. 7B).

4. Discussion

Multiple histological changes in the bladder wall occurred following BOO, including hypertrophy, tissue hypoxia, inflammation, and fibrosis, which were character-

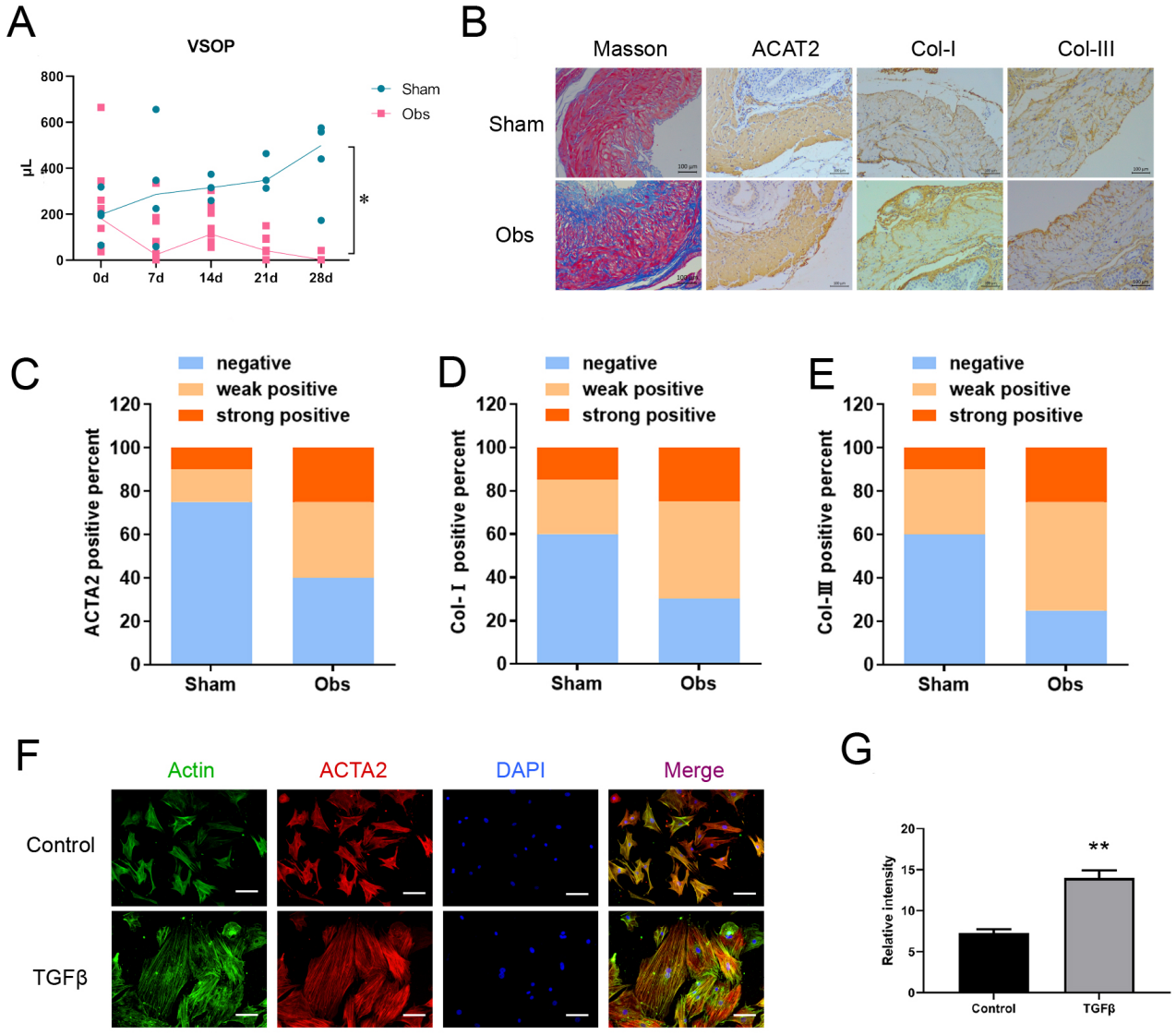

Fig. 1. Bladder function and pathological change following BOO. (A) Voiding behavior was assessed using VSOP. And the results showed that urine volume decreased dramatically in the obstruction group. (B–E) Masson's staining showed more fibrosis, and IHC showed higher expression levels of ACTA2, Col-I, Col-III in the obstruction group. The representative images and IHC positivity statistics are shown. Scale bar = 100 μm. (F,G) TGFβ can induce smooth muscle cell hypertrophy. Scale bar = 100 μm. The data are expressed as the mean ± SEM, and n = 10 for each group in VSOP, n = 6 for each group in others. *$p < 0.05$; **$p < 0.01$.

ized by increasing extracellular matrix [11]. In our study, we confirmed the bladder dysfunction with urine volume change post-obstruction, and the downtrend continued for four weeks (Fig. 1A). Collagen type I served as one of the extracellular matrix produced by fibroblasts, mediated by TFGβ, and contributed to fibrosis [12]. Through Masson's staining, we observed fibrosis occurred, which was also identified with the increase of Col-I, Col-III, and ACTA2 (Fig. 1B–E). Hypertrophy is an important pathological change after BOO. It was observed in smooth muscle cells treated with TGFβ, which was labeled with Actin and ACTA2 (Fig. 1F,G). *In vivo* and *in vitro* results proved bladder fibrosis following BOO.

Fibrosis involves the hyperproliferation and activation of fibroblasts, leading to abnormal accumulation of ECM [13]. This process can be triggered by mechanical and biochemical factors such as hydrostatic pressure, stretching force, fluid shear stress, and ECM stiffness, which promote tissue repair and cell adhesion [14]. Current study has indicated that ADRB2 and ADRB3 were upregulated by hydrostatic pressure via EPAC/SMAD2/FN and EPAC/SMAD3/COL1 pathways, contributing to bladder fibrosis in BOO models [4]. Another study showed that the upregulation of PDE5 can be detected following BOO, modulated by nitric oxide synthase (NOS), and leads to bladder smooth muscle hypertrophy and hyperpla-

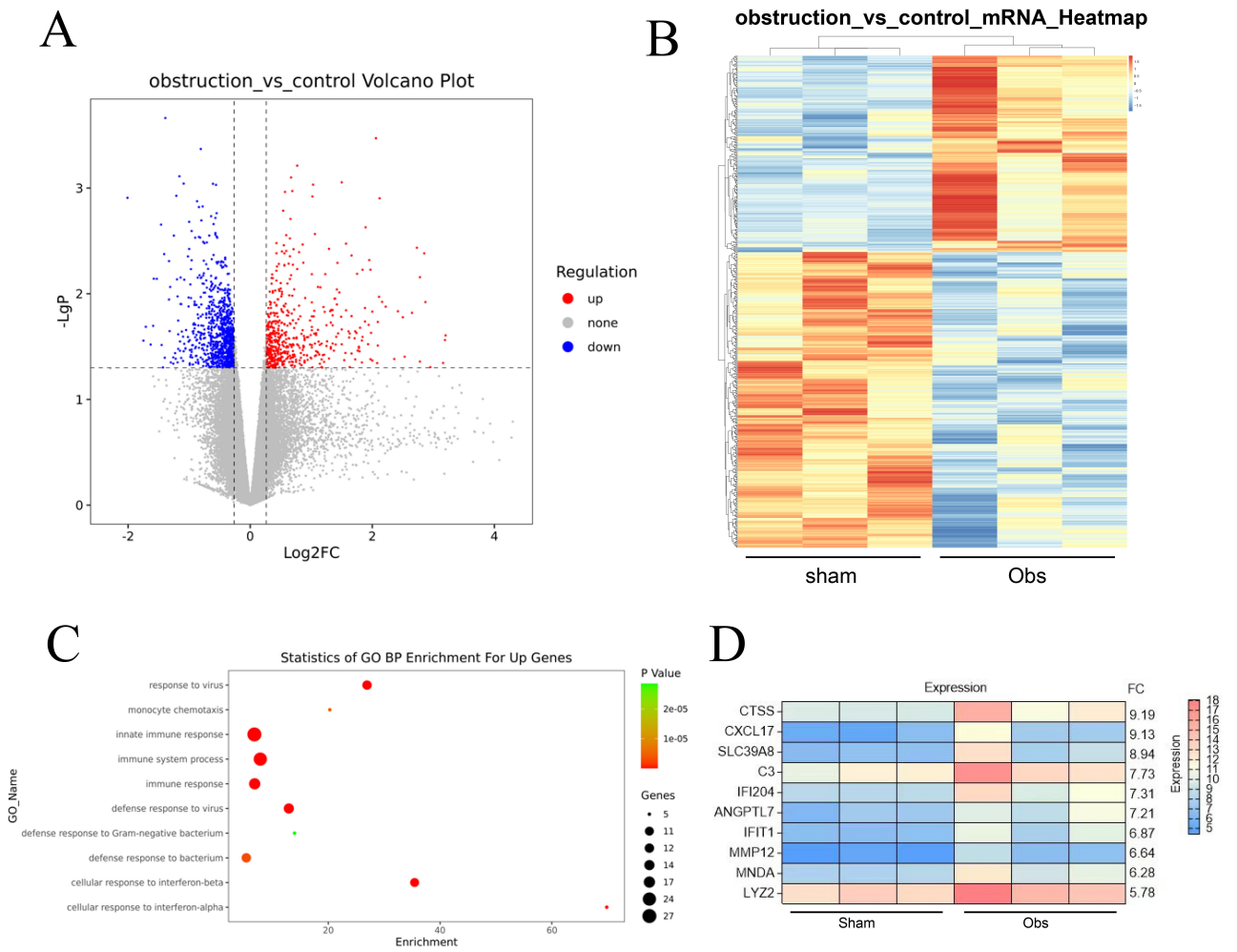

Fig. 2. Gene expression analysis for BOO and sham mice. (A) Volcano Plot shows the distribution of differential genes between the control group and obstruction group. (B) Hierarchical Clustering was done for differentially expressed genes and displayed in the form of heatmap. (C) Gene Ontology (GO) analysis of the main functions of the genes upregulated in the Obs group. (D) The top ten most significantly upregulated genes in the Obs group. $p < 0.05$, $|FC| > 1.2$.

sia [15]. Although research in this area is abundant, therapeutic strategies remain insufficient. In our study, we carried out a microarray probe to detect the BOO mice bladder and found the three genes with the highest differential expression. Compared with controls, a total of 541 genes were upregulated and 943 genes were downregulated in BOO mice (Fig. 2A,B). Furthermore, we subjected the differential genes to GO analysis and the results indicated that innate immune response, immune system process, and cellular response to interferon-beta are the major functions of upregulated genes (Fig. 2C). The top ten most significantly upregulated genes were selected (Fig. 2D), and we combined the results of the GO analysis with literature reports and subjected them to Kyoto Encyclopedia of Genes and Genomes (KEGG) analysis. Immune response-associated genes CTSS, CXCL17, and ANGPTL7 were identified as candidate genes. Among the top ten genes, CTSS, CXCL17, and ANGPTL7 showed the highest differential expression (Fig. 3A). From other studies, we found CTSS is associated with the fibrosis process in other organs, combining with our results that CTSS showed the highest elevation in BOO mice bladders and TGFβ-treated SMCs (Fig. 3B–E), we selected CTSS as the target protein in further study.

CTSS is short for cathepsin S, which is a member of the cysteine cathepsin protease family [16]. It is defined by proteolytic activity and is characterized as restricted tissue expression, associated with antigen-presenting cells, and retains activity at a neutral pH [17–20]. In our study, we detected the overexpression of CTSS following obstruction. Due to its ability to respond to inflammatory stimuli and participate in antigen presentation, CTSS can serve as a target in immunological disorders, allergic inflammation, and asthma [21]. In some studies, CTSS has been found to be expressed in both the upper and lower airways of cystic fibrosis patients, which contributes to the destruction of lung

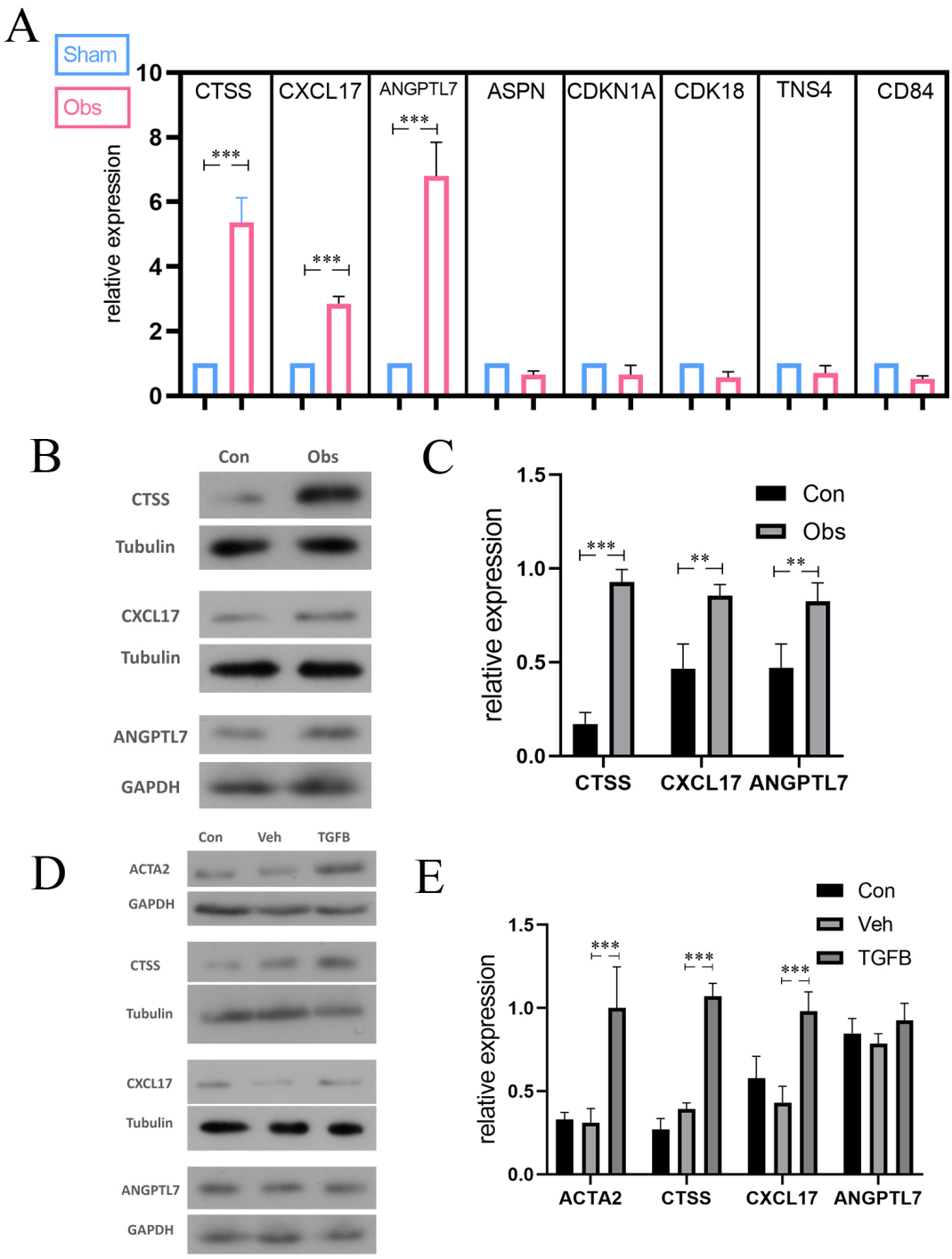

Fig. 3. The differential expression of selected gene or protein following BOO *in vivo* or *in vitro*. (A) qPCR test results in genes selected from microarray result, and CTSS, CXCL17, and ANGPTL7 identified as candidate genes in the following verification. (B,C) the expression of CTSS, CXCL17, ANGPTL7 in mice model. (D,E) the expression of ACTA2, CTSS, CXCL17, ANGPTL7 in smooth muscle cells. The protein levels of CTSS and CXCL17 were upregulated *in vivo* and *in vitro*. But the expression of ANGPTL17 was only significantly elevated *in vitro*. The data are expressed as the mean ± SEM, and n = 6 for each group. $^{**}p < 0.01$; $^{***}p < 0.001$.

elasticity. Elevated protease/anti-protease-ratios contribute to damage of airway tissue and premature death in the inherited disease [22]. CTSS is engaged in the activation of epithelial sodium channels (ENaC) and cleavage of host defense proteins, including surfactants and LL-37, in cystic fibrosis patients [23]. Furthermore, CTSS can be a potential biomarker predicting the disease progression in idiopathic pulmonary fibrosis patients. The rise of cystatin C might trigger the development of lung fibrosis by impairing collagenolytic activity of cysteine cathepsins [24]. Based on

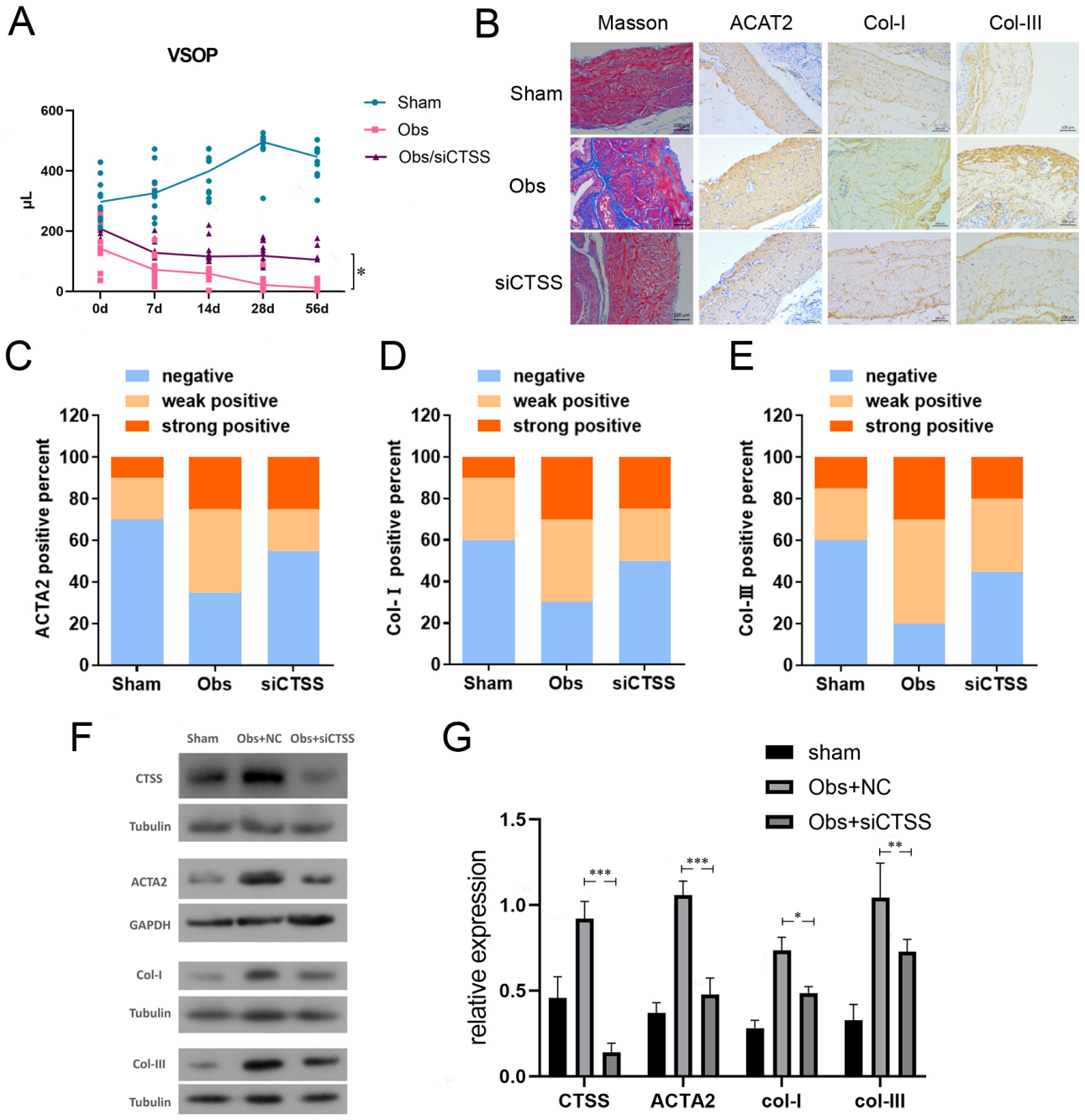

Fig. 4. Downregulation of CTSS improved bladder function and bladder fibrosis after BOO. (A) VSOP showed that bladder function of the Obs/siCTSS group was improved since the 28th day after obstruction, compared with control. (B–E) Downregulation of CTSS improved bladder fibrosis in Masson's staining and IHC. Representative images and IHC positivity statistics are shown. Scale bar = 100 μm. (F,G) Downregulation of CTSS decreased the expression level of ACTA2, Col-I, and Col-III in western blotting. The data are expressed as the mean ± SEM, and n = 10 for each group in VSOP, n = 6 for each group in others. $*p < 0.05$; $**p < 0.01$; $***p < 0.001$.

all these studies, we predicted that CTSS is more likely to be associated with the bladder fibrosis process following BOO among the three genes. We confirmed that after the down-regulation of cathepsin S with siRNA, bladder function and bladder fibrosis were improved compared with control (Fig. 4A–G). To imitate the realistic microenvironment, we co-cultured SMCs and monocyte/macrophages and stimulated them with TGFβ. CTSS and ACTA2 increased in both smooth muscle cells and the co-culture group (Fig. 5A,B). ACTA2's dramatic elevation can only be reduced obviously in the co-cultured group when CTSS is inhibited (Fig. 5C,D). This result confirms that the role

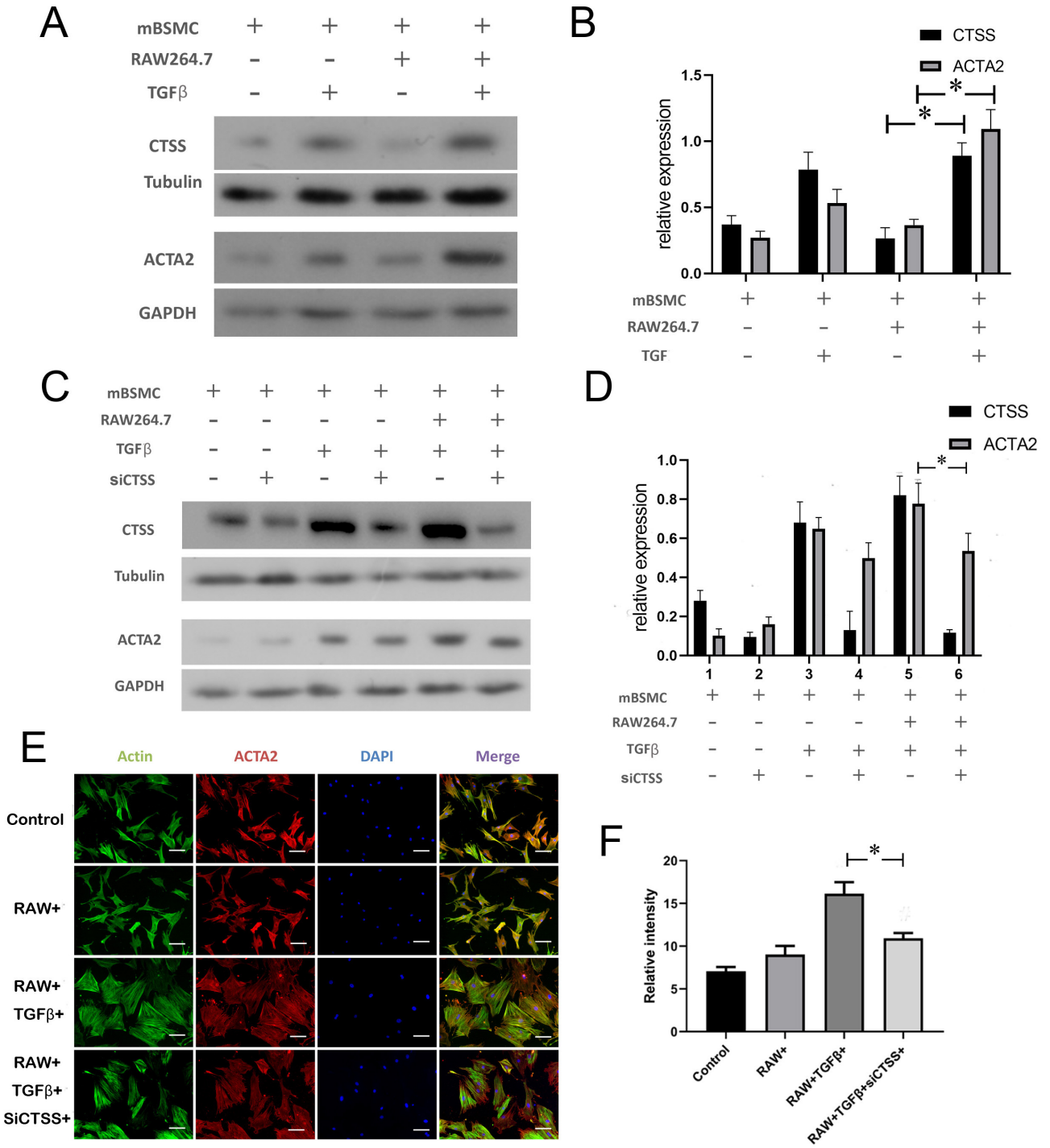

Fig. 5. CTSS contributed to hypertrophy in smooth muscle cells when co-cultured with monocytes. (A,B) The expression level of CTSS and ACTA2 with TGFβ stimulation. (C,D) The expression level of CTSS and ACTA2 with CTSS downregulation. (E,F) Downregulation of CTSS inhibited hypertrophy induced by TGFβ in smooth muscle cells/monocytes. Scale bar = 100 µm. The data are expressed as the mean ± SEM, and n = 6 for each group. *$p < 0.05$.

of CTSS in bladder smooth muscle cell hypertrophy requires the involvement of immune cells. We also confirmed that CTSS contributed to TGFβ-induced hypertrophy of smooth muscle cells, even when co-cultured with macrophages (Fig. 5E,F).

IL-6 is maintained at low serum levels in health and dramatically increases inflammation events [25]. IL-6 activates its target cells by binding to the IL-6R, which is mainly expressed on hepatocytes and different leukocyte subsets such as T cells, B cells, monocyte/macrophages,

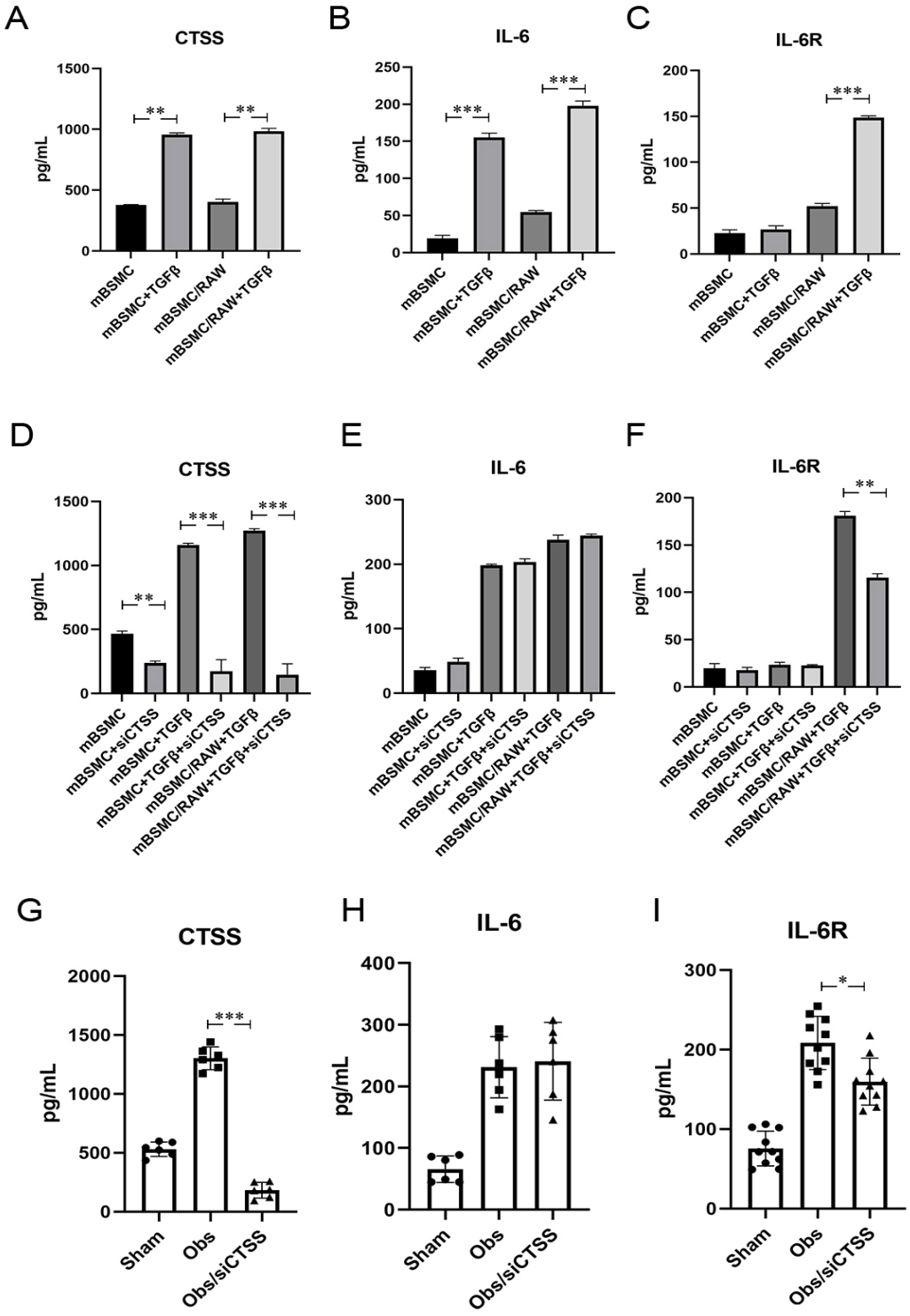

Fig. 6. CTSS activated CTSS/sIL-6R/IL-6 signal pathway after BOO. (A–C) TGFβ induced expression change of CTSS, IL-6, sIL-6R *in vitro*. The expression levels of CTSS and IL-6 both increased in mBSMC and the mBSMC/RAW group stimulated by TGFβ, while IL-6R was only evaluated in the mBSMC/RAW group stimulated by TGFβ. (D–F) Downregulation of CTSS affected the expression change of IL-6, sIL-6R induced by TGFβ *in vitro*. sIL-6R expression decreased significantly only in the stimulated co-cultured group treated with siCTSS. (G–I) Downregulation of CTSS affected the expression change of IL-6, sIL-6R induced by BOO *in vivo*. The data are expressed as the mean $\pm$ SEM, and n = 10 for each group in the IL-6R test *in vivo*, n = 6 for each group in others. *$p < 0.05$; **$p < 0.01$; ***$p < 0.001$.

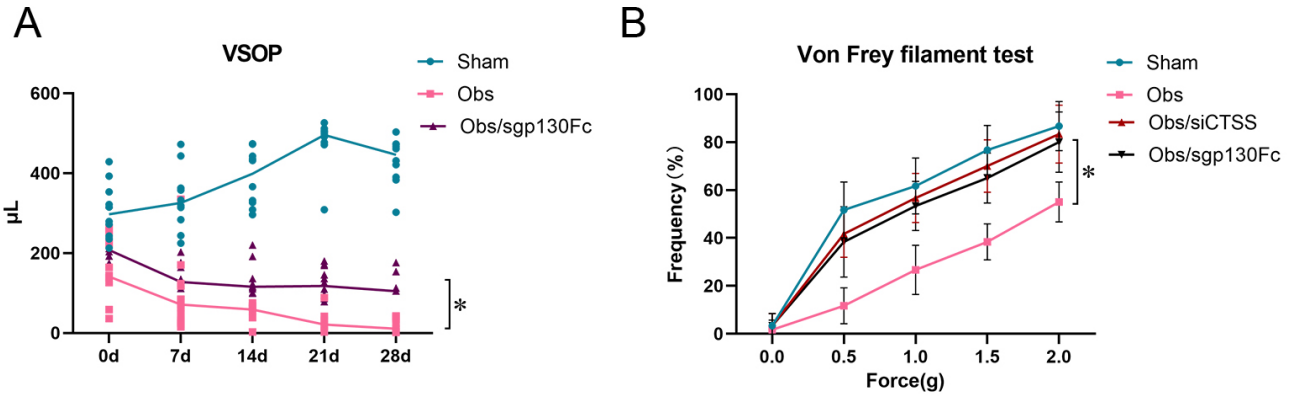

Fig. 7. CTSS affected bladder function through CTSS/sIL-6R/IL-6 trans-signaling after BOO. (A) VSOP showed bladder function was improved when CTSS/sIL-6R/IL-6 trans-signaling was blocked by sgp130FC. (B) Von Frey filament test showed bladder sensibility was improved when CTSS/sIL-6R/IL-6 trans-signaling or CTSS was blocked by sgp130FC or siCTSS. The data are expressed as the mean ± SEM, and n = 6 for each group. *$p < 0.01$.

megakaryocytes, and neutrophils. IL-6 is associated with fibrosis diseases via binding sIL-6R and initiating IL-6 trans-signaling [26]. In a recent study, IL-6 trans-signaling contributes to renal fibrosis [27]. To investigate whether IL-6 trans-signaling participates in bladder fibrosis and how CTSS affects bladder smooth muscle cells, we carried out *in vitro* experiments and tested the cell supernatant. The results indicated that both the smooth muscle cells group and the co-cultured group stimulated by TGFβ showed increased release of IL-6, but sIL-6R only changed in the co-cultured group (Fig. 6A–C). Furthermore, inhibiting CTSS expression reduced only sIL-6R release, which verified that CTSS is directly associated with the cleaving and releasing of sIL-6R in this process (Fig. 6D–F). However, IL-6 was not altered by CTSS, which indicated that IL-6 participated in fibrosis by forming a complex, but it was not directly affected by CTSS. These results were also echoed in the animal BOO model (Fig. 6G–I). Furthermore, it was confirmed through blockade using an IL-6 trans-signaling inhibitor that bladder dysfunction after BOO was mediated by IL-6 trans-signaling (Fig. 7A,B).

5. Conclusion

In summary, bladder fibrosis is a common pathological change after BOO, which is characterized by overexpression of CTSS. In this process, CTSS cleaves IL-6R on the immune cells' surface and forms sIL-6R. Binding with IL-6, sIL-6R participates in IL-6 trans-signaling activity and initiates bladder fibrosis. Thus, CTSS can be identified as a potential therapeutic target of BOO in further studies.

6. Study Limitations

Although we have proposed that CTSS promotes the progression of bladder fibrosis by cleaving IL-6R to form sIL-6R, thereby initiating the next stage through the formation of a CTSS/IL-6/sIL-6R complex, the deeper mechanisms—such as downstream signaling pathways, the cleavage site of IL-6R, and the relationship between downstream signaling pathways and IL-6R cleavage—remain insufficiently explored. In our further studies, we observed that adding CTSS protein to a co-culture cell system increased the phosphorylation levels of Stat3 and Stat6 (**Supplementary Fig. 2**). While it is well known that factors like TGFβ can activate the Stat pathway in immune cells, our research demonstrates that CTSS involvement in the co-culture system can also activate this pathway. Therefore, in the next phase of research, the Stat pathway could serve as a key target to further investigate the mechanism by which CTSS cleaves IL-6R on the surface of immune cells. On the other hand, this study focused on the 28-day time point after BOO. However, BOO-induced damage often worsens and evolves over time. Thus, longer damage cycles will also be a key focus in our next stage of research.

Abbreviations

BPH, Benign prostate hyperplasia; BOO, Bladder outlet obstruction; CTSS, Cathepsin S; CXCL17, C-X-C Motif Chemokine Ligand 17; ANGPTL7, Angiopoietin Like 7; IL-6, Interleukin-6; IL-6R, Interleukin-6 receptor; LUTS, Lower urinary tract symptoms; ECM, Extracellular matrix; BSMC, Bladder smooth muscle cell; TGFβ, Transforming growth factor-beta; VSOP, Void Stain on Paper; ACTA2, Anti-alpha smooth muscle Actin 2; ENaC, Epithelial sodium channels.

Availability of Data and Materials

The datasets used or analyzed during the current study are available from the corresponding authors on reasonable request.

Author Contributions

LW, TS and MY designed the experiments. MY, XL, HW, and TS carried out the experiments, analyzed the experimental results and wrote the manuscript. All authors contributed to editorial changes in the manuscript. All authors read and approved the final manuscript. All authors have participated sufficiently in the work and agreed to be accountable for all aspects of the work.

Ethics Approval and Consent to Participate

All procedures involving animals in this study complied with the NIH Guide for the Care and Use of Laboratory Animals and were approved by the Animal Care and Use Committee of Tianjin Medical University (approval No. IRB2024-DWFL-173).

Acknowledgment

We would like to express our gratitude to all those who helped me during the writing of this manuscript and thanks to all the peer reviewers for their opinions and suggestions.

Funding

This research was supported by The National Key Research and Development Program of China [2021YFC2009300, 2021YFC2009305], the National Natural Science Foundation of China [82203670] and the Tianjin Medical University General Hospital Young Technical Backbone Program [GG-202407].

Conflict of Interest

The authors declare no conflict of interest.

Supplementary Material

Supplementary material associated with this article can be found, in the online version, at https://doi.org/10.31083/FBL45355.

References

[1] D'Silva KA, Dahm P, Wong CL. Does this man with lower urinary tract symptoms have bladder outlet obstruction?: The Rational Clinical Examination: a systematic review. JAMA. 2014; 312: 535–542. https://doi.org/10.1001/jama.2014.5555.

[2] Rademakers KLJ, van Koeveringe GA, Oelke M. Detrusor underactivity in men with lower urinary tract symptoms/benign prostatic obstruction: characterization and potential impact on indications for surgical treatment of the prostate. Current Opinion in Urology. 2016; 26: 3–10. https://doi.org/10.1097/MOU.0000000000000246.

[3] Metcalfe PD, Wang J, Jiao H, Huang Y, Hori K, Moore RB, *et al*. Bladder outlet obstruction: progression from inflammation to fibrosis. BJU International. 2010; 106: 1686–1694. https://doi.org/10.1111/j.1464-410X.2010.09445.x.

[4] Lai J, Chen G, Su H, He Q, Xiao K, Liao B, *et al*. β-Adrenoceptor Signaling Activation Improves Bladder Fibrosis by Inhibiting Extracellular Matrix Deposition of Bladder Outlet Obstruction. Frontiers in Bioscience (Landmark Edition). 2024; 29: 336. https://doi.org/10.31083/j.fbl2909336.

[5] Gheinani AH, Kiss B, Moltzahn F, Keller I, Bruggmann R, Rehrauer H, *et al*. Characterization of miRNA-regulated networks, hubs of signaling, and biomarkers in obstruction-induced bladder dysfunction. JCI Insight. 2017; 2: e89560. https://doi.org/10.1172/jci.insight.89560.

[6] Wang W, Xiao D, Lin L, Gao X, Peng L, Chen J, *et al*. Antifibrotic Effects of Tetrahedral Framework Nucleic Acids by Inhibiting Macrophage Polarization and Macrophage-Myofibroblast Transition in Bladder Remodeling. Advanced Healthcare Materials. 2023; 12: e2203076. https://doi.org/10.1002/adhm.202203076.

[7] Smyth P, Sasiwachirangkul J, Williams R, Scott CJ. Cathepsin S (CTSS) activity in health and disease - A treasure trove of untapped clinical potential. Molecular Aspects of Medicine. 2022; 88: 101106. https://doi.org/10.1016/j.mam.2022.101106.

[8] Yoo Y, Choi E, Kim Y, Cha Y, Um E, Kim Y, *et al*. Therapeutic potential of targeting cathepsin S in pulmonary fibrosis. Biomedicine & Pharmacotherapy = Biomedecine & Pharmacotherapie. 2022; 145: 112245. https://doi.org/10.1016/j.biopha.2021.112245.

[9] Yao X, Cheng F, Yu W, Rao T, Li W, Zhao S, *et al*. Cathepsin S regulates renal fibrosis in mouse models of mild and severe hydronephrosis. Molecular Medicine Reports. 2019; 20: 141–150. https://doi.org/10.3892/mmr.2019.10230.

[10] Austin JC, Chacko SK, DiSanto M, Canning DA, Zderic SA. A male murine model of partial bladder outlet obstruction reveals changes in detrusor morphology, contractility and Myosin isoform expression. The Journal of Urology. 2004; 172: 1524–1528. https://doi.org/10.1097/01.ju.0000138045.61378.96.

[11] Siregar S, Herlambang MS, Reza M, Mustafa A, Stefanus D. Role of human adipose-derived stem cells (hADSC) on TGF-β1, type I collagen, and fibrosis degree in bladder obstruction model of Wistar rats. BMC Urology. 2022; 22: 69. https://doi.org/10.1186/s12894-022-01019-2.

[12] Kendall RT, Feghali-Bostwick CA. Fibroblasts in fibrosis: novel roles and mediators. Frontiers in Pharmacology. 2014; 5: 123. https://doi.org/10.3389/fphar.2014.00123.

[13] Mehjabin A, Kabir M, Micolucci L, Akhtar MM, Mollah AKMM, Islam MS. MicroRNA in Fibrotic Disorders: A Potential Target for Future Therapeutics. Frontiers in Bioscience (Landmark Edition). 2023; 28: 317. https://doi.org/10.31083/j.fbl2811317.

[14] Di XP, Jin X, Ai JZ, Xiang LY, Gao XS, Xiao KW, *et al*. YAP/Smad3 promotes pathological extracellular matrix microenviroment-induced bladder smooth muscle proliferation in bladder fibrosis progression. MedComm. 2022; 3: e169. https://doi.org/10.1002/mco2.169.

[15] He W, Xiang H, Liu D, Liu J, Li M, Wang Q, *et al*. Changes in the expression and function of the PDE5 pathway in the obstructed urinary bladder. Journal of Cellular and Molecular Medicine. 2020; 24: 13181–13195. https://doi.org/10.1111/jcmm.15926.

[16] Wilkinson RDA, Williams R, Scott CJ, Burden RE. Cathepsin S: therapeutic, diagnostic, and prognostic potential. Biological Chemistry. 2015; 396: 867–882. https://doi.org/10.1515/hsz-2015-0114.

[17] Turk V, Stoka V, Vasiljeva O, Renko M, Sun T, Turk B, *et al*. Cysteine cathepsins: from structure, function and regulation to new frontiers. Biochimica et Biophysica Acta. 2012; 1824: 68–88. https://doi.org/10.1016/j.bbapap.2011.10.002.

[18] Turnsek T, Kregar I, Lebez D. Acid sulphydryl protease from calf lymph nodes. Biochimica et Biophysica Acta. 1975; 403: 514–520. https://doi.org/10.1016/0005-2744(75)90079-0.

[19] Maciewicz RA, Etherington DJ. A comparison of four cathepsins (B, L, N and S) with collagenolytic activity from rabbit spleen. The Biochemical Journal. 1988; 256: 433–440. https://doi.org/10.1042/bj2560433.

[20] Chapman HA, Riese RJ, Shi GP. Emerging roles for cysteine proteases in human biology. Annual Review of Physiology. 1997; 59: 63–88. https://doi.org/10.1146/annurev.physiol.59.1.63.

[21] Cimerman N, Brguljan PM, Krasovec M, Suskovic S, Kos J. Circadian and concentration profile of cathepsin S in sera from healthy subjects and asthmatic patients. Pflugers Archiv: European Journal of Physiology. 2001; 442: R204–6. https://doi.org/10.1007/s004240100026.

[22] Hentschel J, Fischer N, Janhsen WK, Markert UR, Lehmann T, Sonnemann J, *et al*. Protease-antiprotease imbalances differ between Cystic Fibrosis patients' upper and lower airway secretions. Journal of Cystic Fibrosis: Official Journal of the European Cystic Fibrosis Society. 2015; 14: 324–333. https://doi.org/10.1016/j.jcf.2014.09.003.

[23] Taggart CC, Greene CM, Smith SG, Levine RL, McCray PB, Jr, O'Neill S, *et al*. Inactivation of human beta-defensins 2 and 3 by elastolytic cathepsins. Journal of Immunology (Baltimore, Md.: 1950). 2003; 171: 931–937. https://doi.org/10.4049/jimmunol.171.2.931.

[24] Kasabova M, Joulin-Giet A, Lecaille F, Saidi A, Marchand-Adam S, Lalmanach G. Human cystatin C: a new biomarker of idiopathic pulmonary fibrosis? Proteomics. Clinical Applications. 2014; 8: 447–453. https://doi.org/10.1002/prca.201300047.

[25] Hirano T. IL-6 in inflammation, autoimmunity and cancer. International Immunology. 2021; 33: 127–148. https://doi.org/10.1093/intimm/dxaa078.

[26] Gunes A, Schmitt C, Bilodeau L, Huet C, Belblidia A, Baldwin C, *et al*. IL-6 Trans-Signaling Is Increased in Diabetes, Impacted by Glucolipotoxicity, and Associated With Liver Stiffness and Fibrosis in Fatty Liver Disease. Diabetes. 2023; 72: 1820–1834. https://doi.org/10.2337/db23-0171.

[27] Chen W, Yuan H, Cao W, Wang T, Chen W, Yu H, *et al*. Blocking interleukin-6 trans-signaling protects against renal fibrosis by suppressing STAT3 activation. Theranostics. 2019; 9: 3980–3991. https://doi.org/10.7150/thno.32352.